82–96 *Nucleic Acids Research, 2010, Vol. 38, No. 1* *Published online 29 October 2009*
doi:10.1093/nar/gkp873

Two modules in the BRC repeats of BRCA2 mediate structural and functional interactions with the RAD51 recombinase

Eeson Rajendra and Ashok R. Venkitaraman*

The Medical Research Council Cancer Cell Unit, Hutchison/MRC Research Centre, Hills Road, Cambridge, CB2 0XZ, UK

Received August 14, 2009; Revised September 30, 2009; Accepted October 1, 2009

ABSTRACT

The breast and ovarian cancer suppressor protein BRCA2 controls the RAD51 recombinase in reactions that lead to homologous DNA recombination (HDR). BRCA2 binds RAD51 via eight conserved BRC repeat motifs of approximately 35 amino acids, each with a varying capacity to bind RAD51. BRC repeats both promote and inhibit RAD51 assembly on different DNA substrates to regulate HDR, but the structural basis for these functions is unclear. Here, we demarcate two tetrameric clusters of hydrophobic residues in the BRC repeats, interacting with distinct pockets in RAD51, and show that the co-location of both modules within a single BRC repeat is necessary for BRC–RAD51 binding and function. The two modules comprise the sequence FxxA, known to inhibit RAD51 assembly by blocking the oligomerization interface, and a previously unrecognized tetramer with the consensus sequence LFDE, which binds to a RAD51 pocket distinct from this interface. The LFDE motif is essential in BRC repeats for modes of RAD51 binding both permissive and inhibitory to RAD51 oligomerization. Targeted insertion of point mutations in RAD51 that disrupt the LFDE-binding pocket impair its assembly at DNA damage sites in living cells. Our findings suggest a model for the modular architecture of BRC repeats that provides fresh insight into the mechanisms regulating homologous DNA recombination.

INTRODUCTION

The BRCA2 tumour suppressor is essential for homologous DNA recombination (HDR), a process for the error-free repair of DNA double-stranded breaks (DSBs), in the cells of higher eukaryotes (1,2). BRCA2 orthologues exist in most eukarya, with the notable exception of yeast (3). Their central function during HDR (4) is to control the RAD51 recombinase (5,6), an enzyme conserved in the other kingdoms of life as RecA in eubacteria, or RadA in archaea. RAD51 is indispensable for HDR (7–9), which begins when broken DNA is end-resected to generate ssDNA, upon which RAD51 oligomerizes to form an active nucleoprotein filament. The RAD51 nucleoprotein filament catalyzes strand exchange by invading and pairing with a homologous DNA duplex, used as a template for repair. Several functions have been ascribed to the BRCA2-RAD51 interaction, both *in vivo* and *in vitro*, in regulating these events. They include the sequestration of RAD51 in undamaged cells and its mobilization after damage (10), targeting of RAD51 to DSBs (11), control of RAD51 oligomerization (12,13) and modulation of sequential DNA substrate selection by RAD51, a process that orders the strand exchange reaction itself (14,15).

Two distinct regions in human BRCA2 bind directly to RAD51. Eight BRC repeats, evolutionarily conserved motifs of approximately 35 residues each, distributed in a ~1100 residue region of BRCA2 ($BRCA2_{BRC1\text{-}8}$), are conserved amongst vertebrate orthologues in both their sequence and spacing (16–18). Each of the eight BRC repeats in human BRCA2, despite only subtle sequence variation, exhibits a varying affinity for RAD51 (19–21). BRC repeats, in isolation, or in the context of $BRCA2_{BRC1\text{-}8}$, bind RAD51 complexes on DNA (22,23) and differentially regulate RAD51 assembly on ssDNA versus dsDNA, promoting loading onto ssDNA, whilst concurrently impeding loading onto dsDNA, thereby stimulating strand exchange (14,15). A second, distinct, RAD51-interacting region located at the extreme C-terminus of BRCA2 stabilizes RAD51 oligomeric assemblies *in vitro* both on and off DNA (24,25). However, recent cellular studies suggest that the C-terminal RAD51-binding region is dispensable for the execution of HDR *in vivo,* and instead, coordinates

*To whom correspondence should be addressed. Tel: +44 1223 336901; Fax: +44 1223 763374; Email: arv22@cam.ac.uk

the termination of HDR with entry into mitosis (26). Thus, the binding of BRCA2's BRC repeats to RAD51 may be the primary mode of interaction between the two proteins relevant to HDR.

The structure of a complex between human BRC repeat 4 (BRC4) and the core catalytic domain of RAD51 provides insight into this interaction. BRC4 uses the sequence FHTA (human BRCA2 residues 1524–1527) within the context of a β-hairpin secondary structural motif to directly mimic the inter-subunit oligomerization motif of the RAD51 protein (13). In this mode of interaction, the BRC4-RAD51 interaction is expected to *inhibit* RAD51 oligomerization, consistent with the observations that excess BRC repeat peptides (at $>\sim$3–4 : 1 molar ratios) antagonize RAD51 nucleoprotein filament formation *in vitro* (12) or the formation of RAD51 nuclear foci *in vivo* (13,19). However, it has become clear through later studies that a second mode of BRC–RAD51 interaction also exists, which is *permissive* for RAD51 oligomerization on DNA. At lower stoichiometries of interaction approaching 1 : 1 molar ratios, BRC repeats in isolation or in the context of the entire $BRCA2_{BRC1\text{-}8}$ region, can bind to RAD51 nucleoprotein filaments (22,23), and promote strand exchange reactions *in vitro* (8,23,27). Indeed, recent data suggest that isolated BRC repeats or the $BRCA2_{BRC1\text{-}8}$ fragment promote the stable interaction of RAD51 with ssDNA substrates, whilst inhibiting assembly on dsDNA, and that these opposing activities reinforce one another to favour sequential progression through the steps of HDR (14,15). Thus, biochemical and cellular studies indicate that the BRC repeats of human BRCA2 can interact with RAD51 in modes inhibitory or permissive to RAD51 oligomerization on DNA substrates. However, the structural basis for these seemingly disparate interactions remains unclear.

Here, we have combined structural modelling, biochemistry, cell biology and genetics to address how BRC repeat binding to RAD51 may influence function. We identify two tetrameric motifs for RAD51 binding in the BRC repeats, defining a previously unrecognized motif, LFDE (human BRC4 nomenclature), which is essential for the BRC-RAD51 interaction in BRC repeats of divergent sequence. Although both motifs are required for potent interaction with RAD51, their engagement in structurally discrete binding sites on RAD51, their differential contributions to RAD51 binding by different BRC repeats, and their occurrence within distinct secondary structural motifs of fixed spacing, argue that these sites may constitute distinct binding modes. Consistent with its essential function, abrogation of the LFDE-binding pocket in RAD51 by insertion of point mutations triggers cellular lethality and defective RAD51 assembly at sites of DNA damage. Indeed, we show by structural modeling that the LFDE–RAD51 interaction conserves a salt bridge critical for nucleoprotein filament formation by bacterial RecA, an example of molecular mimicry during evolution, and the second identified at the BRC4–RAD51 interface. Our findings suggest a model in which two discrete modules are used in BRC repeats for unique modes of binding to RAD51, which help to explain their inhibitory and permissive functions during RAD51 oligomerization on DNA substrates. This work provides fresh insight into the mechanism of HDR and its regulation by the BRC repeats of BRCA2.

MATERIALS AND METHODS

Cloning

The mCherry-HsRAD51 expression construct, comprising RAD51 with an N-terminal mCherry fluorophore tag, was a kind gift of Robert Mahen. Site-directed mutagenesis was performed using the Quickchange Site-Directed Mutagenesis Kit (Stratagene). All clones were verified by nucleotide sequencing (Geneservice Ltd). RAD51 was subcloned into pET28a(+), containing an N-terminal 6×His tag fusion, via the NheI–BamHI sites in the multiple cloning site.

Protein purification

Recombinant RAD51, cleaved from GST-RAD51, was used for enzyme-linked immunosorbent assays (ELISA). The bacterial expression plasmid pGex2TK-HsRad51 was a kind gift of Dr Debbie Bates. GST-RAD51 was prepared from *Escherichia coli* BL21 cells using standard affinity purification protocols with glutathione-sepharose 4B beads (Amersham). RAD51 was cleaved from the GST moiety by overnight incubation at 22°C with thrombin protease (Amersham), dialysed into PBS in a Slide-A-Lyser 10 000 MWCO Dialysis Cassette (Pierce) and concentrated using a Vivaspin-15 10 000 MWCO concentrator (Sartorius). Untagged RAD51 used in electrophoretic mobility shift assays (EMSA) and recombinant biotinylated peptide pull downs was a kind gift of Jane Savill. Untagged $RAD51^{R250A}$ was prepared using the same method described for RAD51(23).

Peptides

All peptides were synthesized by Cambridge Research Biochemicals Ltd or Peptide Protein Research Ltd with an N-terminal biotin moiety attached through a 6-aminohexanoic acid spacer, and a C-terminal amide. Peptides were purified to 95% by HPLC, sequence-verified by time-of-flight mass spectrometry and diluted in water (supplemented with 5 mM DTT if containing cysteine residues).

DT40 transfection

All constructs were transfected into $Rad51^{-/-}$/$HsRAD51^{Tet\ off}$ DT40 cells as previously described (28).

Cell viability

Independent DT40 clones were grown and maintained in log phase. Viable cells were enumerated after trypan blue staining using a Beckman Coulter Vicell XR Cell Viability analyzer.

Western blotting

Whole-cell extracts were prepared in ice-cold RIPA buffer, resolved by by SDS–PAGE and immuno-blotted as detailed in Supplementary Methods.

Streptavidin-bead peptide pull-down assay

Pull down of RAD51 using biotinylated BRC peptides was performed as outlined in Supplementary Methods.

ELISA

Competitive ELISA experiments using biotinylated BRC peptides to disrupt the BRC4–RAD51 interaction were performed as outlined in Supplementary Methods.

Sister chromatid exchange assay

The sister chromatid exchange assay in the presence or absence of 50 ng/ml mitomycin C was performed as described previously (29) and in the Supplementary Methods.

Microscopy

Direct mCherry-RAD51 imaging was initially performed on a Zeiss LSM510 Meta confocal microscope and enumerated by automated microscopy on an Olympus ScanR high-content screening microscope as decribed in Supplementary Methods.

EMSA

EMSAs were performed as previously described (15,23). Briefly, RAD51 at 2 μM and BRC repeats at indicated concentrations were pre-incubated in a 10 μl reaction volume on ice for 10 minutes. Preformed complexes were incubated with 6 μM ^{32}P-labeled *Apa*L1-linearised ΦX174 dsDNA (New England Biolabs) in buffer B (40 mM Tris–HCl, pH 7.8, 1 mM $MgCl_2$, 1 mM DTT, 1 mM AMPPNP and 200 mM KCl) at 37°C for a further 60 min. The protein–DNA complexes on dsDNA were resolved by 0.5% agarose gel electrophoresis in TAE buffer at 50 mA for 4 h at 4°C. The dried gels were exposed to a phosphorimager screen and visualized on a FujiFilm FLA-5000 processor.

Statistical analysis

All statistical analyses were performed using GraphPad Prism version 5 for Windows (GraphPad Software).

Structural analysis

All structures were modeled and images prepared using the PyMOL Molecular Graphics System (http://pymol.org/). The numerical solution of the Poisson–Boltzmann equation over the solvent surface of RAD51 was generated using the Adaptive Poisson–Boltzmann Solver (APBS) and is coloured according to the electrostatic potential (−10kT to +10kT) calculated in the absence of BRC4 (30). Solvent accessible surface areas (SASAs) of the RAD51 and BRC4 proteins from 1N0W were calculated using POPSCOMP (31).

Bioinformatics analysis

Sequence alignments were generated using the ClustalW2 alignment program and processed with JalView 2.3 (32,33). Sequences are rendered with the default ClustalX colour scheme, assigning colours to residues if the amino acid profile at the given position is conserved by both residue type and above a minimum threshold of percentage presence.

RESULTS

Two tetrameric clusters of hydrophobic residues in the BRC4 repeat contact RAD51

The high-resolution crystal structure of a fusion protein containing the RecA-homology domain of RAD51 (residues E98-D339) in complex with human BRC repeat 4 (BRC4, BRCA2 residues 1519–1551) has been previously reported (PDB ID: 1N0W) (Figure 1A) (13). The N-terminal domain of RAD51, as well as the linker region connecting it to the core catalytic domain that contains a tetrameric cluster of residues 86-FTTA-89 necessary for RAD51 oligomerization, are both absent from the crystallized RAD51-BRC4 complex. This renders the complex monomeric, and exposes the entire interaction surface necessary and sufficient for BRC4 interaction (13,34).

Crucially, the structure shows that a region of BRC4, 1524-FHTA-1527, positioned within the context of a β-hairpin, binds directly to the oligomerization interface of RAD51. The FHTA motif in the BRC4 peptide occupies two hydrophobic pockets that would, in a RAD51 oligomer, be occupied by the FTTA motif in RAD51 to mediate inter-subunit contact (13). Thus, BRC4 mimics the oligomerization interface in RAD51, suggesting a mechanism for antagonism of RAD51 oligomerization. The FHTA motif of BRC4 is represented in other mammalian BRCA2 and RAD51 homologues as the consensus sequence FxxA, in which the F and A side chains are expected to make contacts with hydrophobic pockets on the core catalytic domain of RAD51.

The C-terminal portion of BRC4 in the BRC4–RAD51 complex, comprising residues I1534-Q1551, constitutes a distinct secondary structural domain, within an α-helical context, that could also be important for interaction with RAD51 (Figure 1). This region makes contacts with RAD51 distant from the oligomerization interface, and in full-length RAD51, would likely cause a steric clash with the N-terminal domain, which is absent from the crystallized complex (22,34).

To dissect the contribution of this second region in BRC4 to the BRC4–RAD51 interaction, we compared the surface properties of BRC4 and RAD51 in their native and co-complexed states (31). The majority of the SASA lost when the proteins interact is hydrophobic (Figure 1B), a common feature in protein–protein interactions (35,36). The effect on RAD51 is less significant because the interaction with BRC4 consumes a smaller proportion of its total surface, but an effect is still observable.

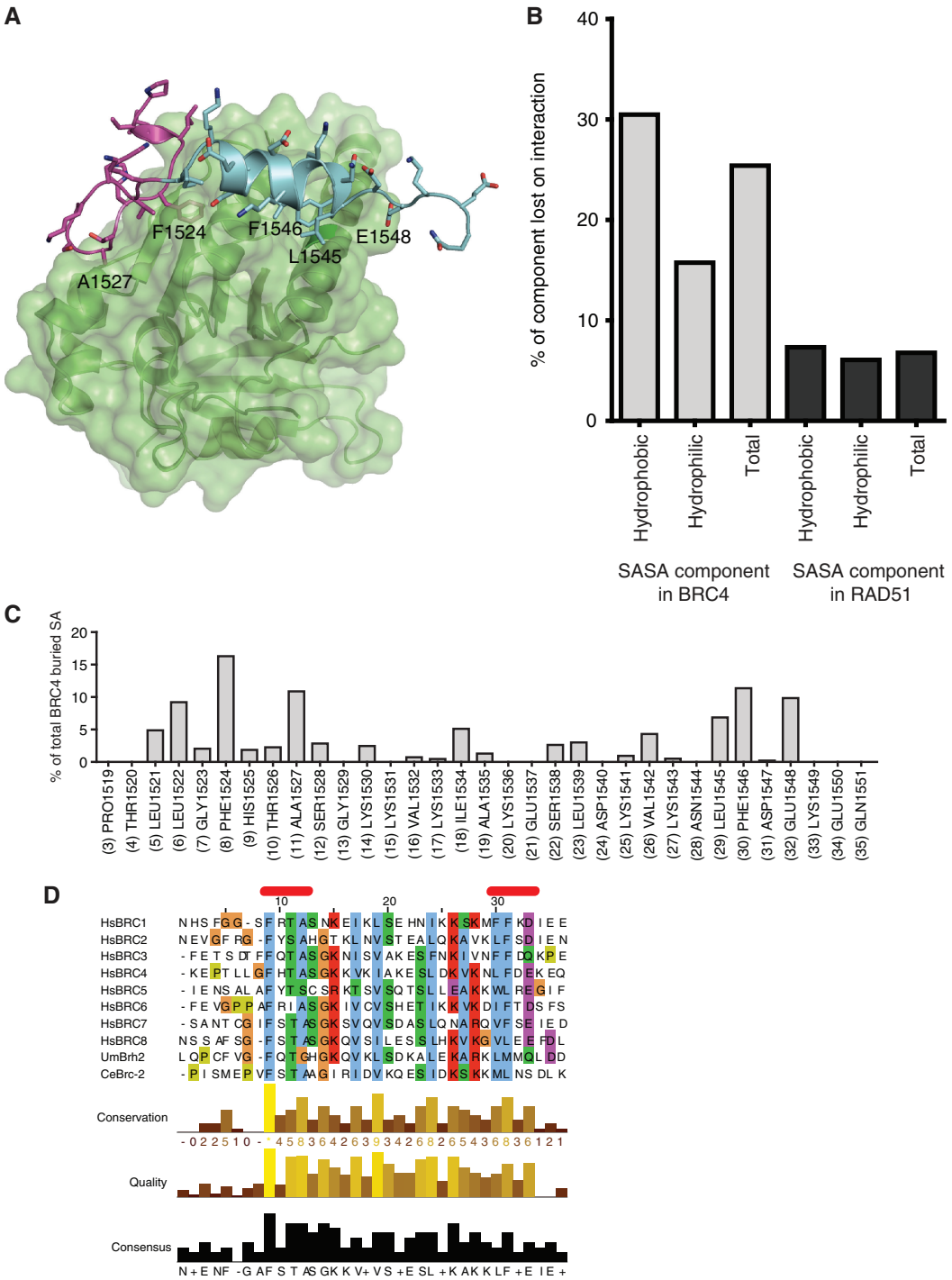

Figure 1. Two distinct hydrophobic motifs within BRC repeats constitute the majority of interaction with RAD51. (**A**) Ribbon representation of the human BRC4-RAD51 interface (PDB ID: 1N0W). The N-terminal BRC4 hairpin (residues 1519–1533) and α-helical C-terminus (residues 1534–1551) are coloured magenta and blue, respectively. RAD51 is in green with a transparent solvent accessible surface.(**B**) Histogram showing the loss of SASA that occurs between unbound and bound BRC4 peptide (grey) on interaction with the core domain of RAD51 and the equivalent effect on RAD51 (black). 25.4% of total SASA on BRC4 is lost of which 30.4% is hydrophobic and only 15.7% is hydrophilic. (**C**) Histogram showing the contribution of each residue in BRC4 to interaction with Rad51, as measured by buried surface area on binding to RAD51. Two BRC4 motifs, FHTA (residues 1524–1527) and LFDE (1545–1548), consist of residues contributing strongly to buried surface area and are clustered around the two most buried residues, F1524 and F1546, that constitute 16.3% and 11.4% of total buried area. (**D**) Sequence alignment of all eight human BRC repeats and the single BRC repeat found in *Caenorhabditis elegans Brc-2* and *Ustilago maydis Brh2*. Both the FHTA and LFDE motifs are strongly conserved by amino acid similarity and spacing in BRC1-8 and the hydrophobic component of the LFDE motif across all BRC repeats.

BRC4 residues contributing to the interaction with RAD51 cluster into two predominantly hydrophobic motifs, each of four residues, which comprise the majority of buried surface area at the RAD51–BRC4 interface (Figure 1C). The first tetrameric cluster has the sequence FHTA (residues 1524–1527); the molecular mimic of the native RAD51 oligomerization sequence 86-FTTA-89. However, a second motif, LFDE (residues 1545–1548), resides in the C-terminus of the BRC4 peptide.

The LFDE motif is conserved in all eight human BRC repeats, with hydrophobic residues in the first and second positions, and either an acidic residue (BRC1, BRC2, BRC4, BRC5–BRC8) or glutamine (BRC3) in the fourth position (Figure 1D). The third position of the tetramer is redundant, in keeping with this residue being solvent-exposed (Figure 1A). Intriguingly, the two initiating hydrophobic residues of the LFDE motif in particular, are conserved not just in all eight human BRC repeats, but even in a BRCA2 orthologue from a simple eukaryote which possesses but a single BRC-repeat (Figure 1D) (3). In comparison, the FHTA tetramer is conserved in seven repeats (but not BRC5) as FxxA, with a threonine residue found at the third position in six of the eight repeats (excepting BRC2 and BRC6), as well as in the FTTA motif native to RAD51.

Both tetrameric clusters are necessary for the BRC–RAD51 interaction

To test whether the BRC4-RAD51 interaction relies on both tetrameric clusters, we developed an ELISA assay, which measured the ability of wild-type or mutant BRC peptides (Table 1) to compete for the interaction between BRC4 peptide (in the solid phase) and recombinant full-length RAD51 (in solution) (Figure 2A). Mutant BRC peptides contained either an F1524E mutation (recapitulating a substitution in the FxxA cluster shown to disrupt RAD51 oligomerization (10)) or the combined substitution of the hydrophobic residues in the LFDE cluster with glutamic acid, and the terminal charged residue with alanine (i.e. L1545E, F1546E, E1548A). For downstream assays, peptides were N-terminally biotinylated; this moiety had no effect on BRC repeat functionality in direct comparison with unconjugated peptides either as a soluble inhibitor or for solid-phase capture of RAD51 (Supplementary Figure S1).

Our findings suggest that the FHTA and LFDE interaction motifs in BRC4 are together necessary for the BRC4–RAD51 interaction. Thus, mutant peptides containing substitutions disrupting the two motifs individually or in combination failed to competitively inhibit the BRC4–RAD51 interaction in the ELISA assay (Figure 2B).

Conversely, conservative substitution with tryptophan of the phenylalanine residues F1524 and F1546, which contribute the majority of buried surface area to interaction with RAD51 (i.e. F1524W and F1546W (Figure 1C)) does not greatly alter the ability of mutant peptides to competitively inhibit the BRC4–RAD51 interaction (Figure 2B). Although the indole moiety of tryptophan is larger than the benzyl group in phenylalanine, structural modelling predicts that it can still be accommodated in both the FHTA- and LFDE-binding pockets of RAD51 (Figure 2C and D, respectively). Moreover, BRC4-derived peptides harbouring single F1524W and F1546W substitutions combined with mutations disrupting the remaining tetrameric motif (i.e. $BRC4^{WE}$ and $BRC4^{EW}$, respectively) fail to competitively inhibit the BRC4–RAD51 interaction. Thus collectively, our results indicate that both the FHTA and LFDE motifs in BRC4 are necessary for interaction with RAD51. These motifs bind to distinct pockets in RAD51, which can be considered interaction hotspots at which the majority of buried surface area is found at residues F1524 and F1546 in BRC4 (37,38).

A chimaeric fusion between BRC4 and BRC5 functionally reconstitutes a potent BRC repeat

An intriguing feature is that each of the human BRC repeats has a varying affinity for RAD51. Most notably, the BRC5 repeat has been shown to have the lowest affinity, in contrast to BRC4 (20,21,39). Despite this,

Table 1. BRC-derived peptides used in this study

Name	Sequence	FxxA	LFDE
BRC4	KEPTLLGFHTASGKKVKIAKESLDKVKNLFDEKEQ	intact	intact
$BRC4^{EF}$	KEPTLLGEHTASGKKVKIAKESLDKVKNLFDEKEQ	mutated	intact
$BRC4^{FE}$	KEPTLLGFHTASGKKVKIAKESLDKVKNEEDAKEQ	intact	mutated
$BRC4^{EE}$	KEPTLLGEHTASGKKVKIAKESLDKVKNEEDAKEQ	mutated	mutated
$BRC4^{EW}$	KEPTLLGEHTASGKKVKIAKESLDKVKNLWDEKEQ	mutated	F to W
$BRC4^{WE}$	KEPTLLGWHTASGKKVKIAKESLDKVKNEEDAKEQ	F to W	mutated
$BRC4^{WW}$	KEPTLLGWHTASGKKVKIAKESLDKVKNLWDEKEQ	F to W	F to W
$BRC4^{E1548A}$	KEPTLLGFHTASGKKVKIAKESLDKVKNLFDAKEQ	intact	E1548A
BRC5	IENSALAFYTSCSRKTSVSQTSLLEAKKWLREGIF	intact	intact
BRC^{45}	KEPTLLGFHTASGKKVKVSQTSLLEAKKWLREGIF	BRC4	BRC5
BRC^{54}	IENSALAFYTSCSRKTSIAKESLDKVKNLFDEKEQ	BRC5	BRC4
BRC^{4A}	KEPTLLGFHTASGKKVK	FHTA (BRC4)	
BRC^{5A}	IENSALAFYTSCSRKTS	FYTS (BRC5)	
BRC^{4B}	IAKESLDKVKNLFDEKEQ		LFDE (BRC4)
BRC^{5B}	VSQTSLLEAKKWLREGIF		WLRE (BRC5)

All peptides are N-terminal biotinylated and are based on the core 35 amino acid register of BRC4

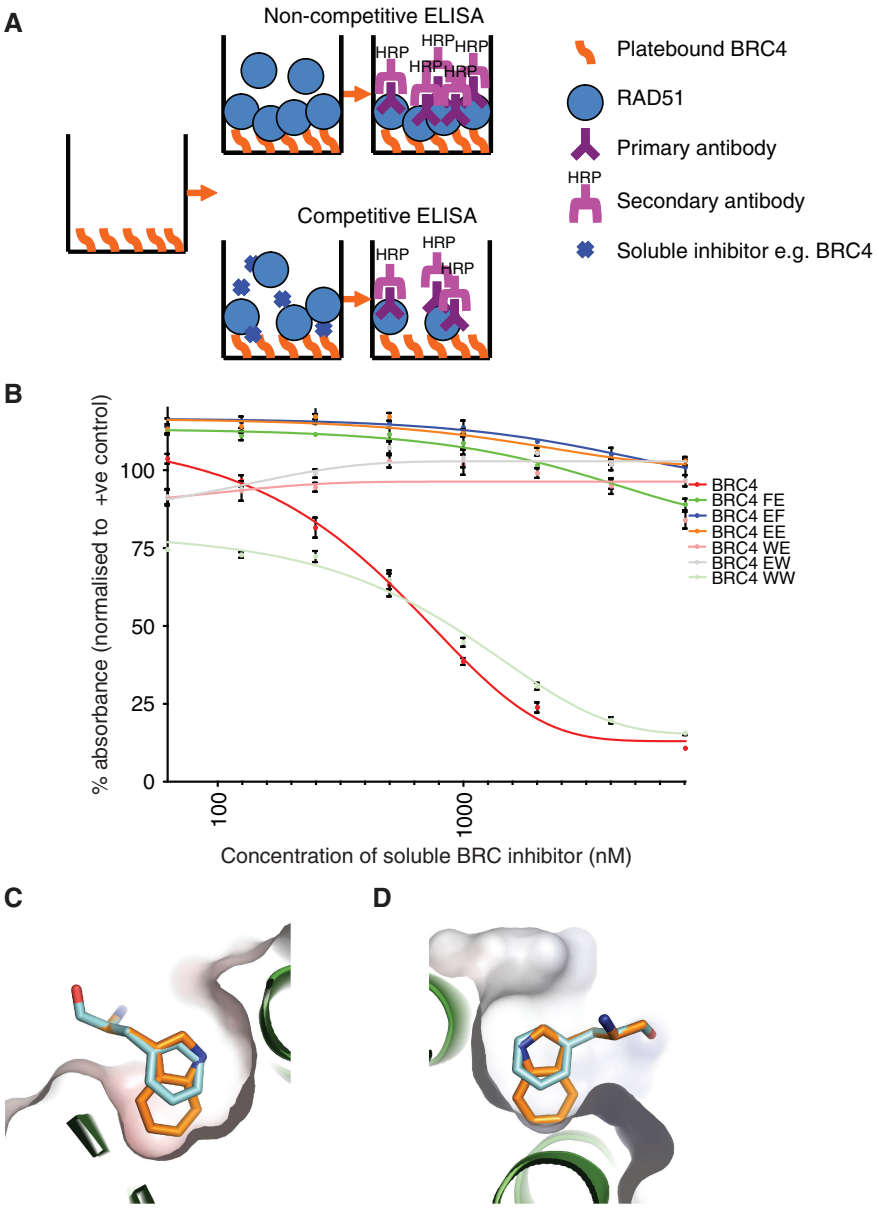

Figure 2. Inhibition of the interaction between BRC4 and RAD51 requires that both binding motifs be intact in BRC4. (**A**) Schematic of the ELISA assay used to detect BRC–RAD51 interaction, and its disruption by soluble peptides. (**B**) In a competitive ELISA assay, detecting disruption of the solid phase BRC4 and Rad51 interaction by soluble peptides, only peptides containing both and intact FHTA and LFDE motif show inhibitor behaviour. A peptide containing both F1524 and F1546 mutated to tryptophan retains similar behaviour, but substitution of phenylanine to tryptophan in either position individually is unable to reconstitute inhibitory behaviour of a peptide when the other motif is disrupted. Values are expressed as the mean percentage absorbance and SEM for triplicate data sets normalized to the positive control without soluble inhibitor. (**C** and **D**) Representations of the BRC4–RAD51 interface with the addition of the solvent accessible surface on Rad51. Clipping planes reveal the two hydrophobic pockets bound by BRC4 phenylalanines F1524 (C) and F1546 (D) (cyan, stick) and that they can both be mutated, without steric or electrostatic clash, to tryptophan (orange, stick). The indole side chains of tryptophan adopt a similar binding pose to the benzyl side chains of the phenylalanines.

BRC5 contains the LFDE-like motif 1692-WLRE-1695. This might conceivably confer stronger binding than the native LFDE sequence in BRC4, since the substitution could contribute more buried surface area into the large hydrophobic pocket in RAD51. The native BRC5 tetrameric cluster WLRE has two hydrophobic residues in the first and second positions and a glutamate in the fourth. We reasoned that residues W1692 and L1693 in the BRC5 peptide could also be accommodated in the same pocket used by BRC4 residues L1545 and F1546. W1692 is in the first position in the BRC5 tetrameric cluster but F1546, which can be functionally reconstituted by a tryptophan (Figure 2B and D), is in the second position of the LFDE cluster in BRC4 (Figure 1D).

To test this hypothesis, we first synthesized peptides spanning residues 1–17 and 18–35 from the 35-residue

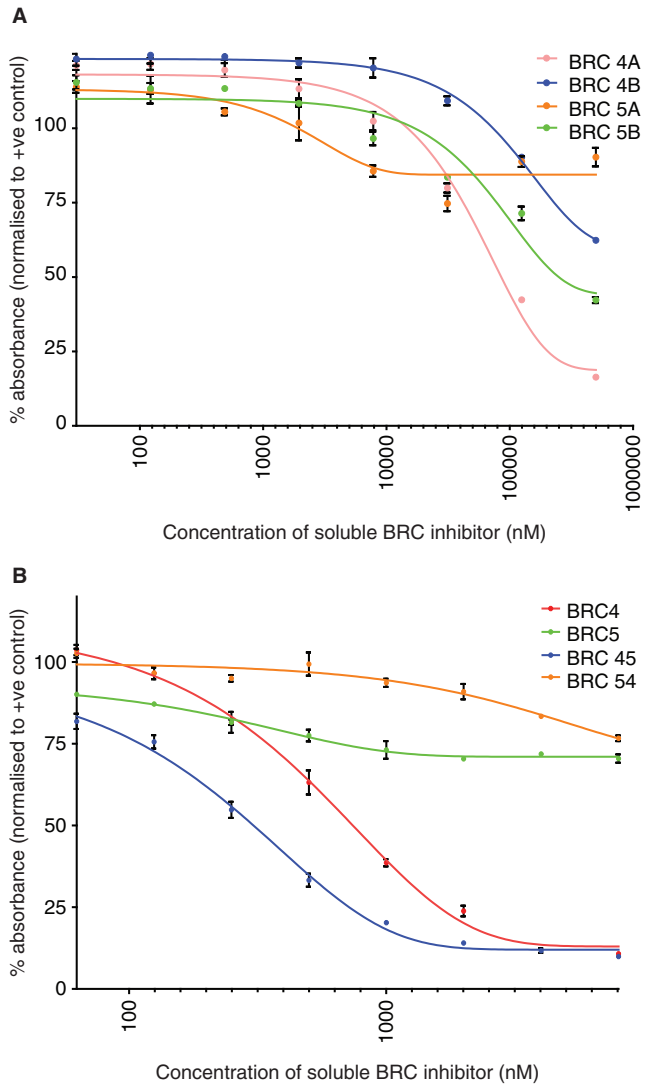

Figure 3. A chimaeric fusion peptide of the N-terminus of BRC4 and C-terminus of BRC5 reconstitutes a functional BRC4-like peptide. (**A**) The inhibitory potential of isolated N- and C-terminal peptides from BRC4 and BRC5: BRC^{4A}, BRC^{4B}, BRC^{5A} and BRC^{5B} (see Table 1 for sequence). BRC^{4A} and BRC^{4B} alone have inhibitory potential (although a significantly lower potency than full length BRC4, see Figures 2B and 3B for comparison). The BRC^{5B} peptide, containing the C-terminus of BRC5, but not BRC^{5A}, has inhibitory potential also. (**B**) A peptide containing a fusion of the N-terminal FHTA motif of BRC4 and the C-terminal WLRE motif of BRC5 acts as a potent soluble inhibitor of the BRC4–RAD51 interaction. Peptides corresponding to BRC5 and an inverse fusion of the N-terminus of BRC5 and the C-terminus of BRC4 fail to show significant inhibitory behaviour.

BRC4 or BRC5 peptides, using the sequence register shown in Figure 1D. The 17-mer N-terminal BRC4 peptide BRC^{4A} (containing the 1524-FHTA-1527 motif) was able to compete with a modest potency against full-length BRC4 for RAD51 binding (Figure 3A), as did the 18-mer BRC4 or BRC5 C-terminal peptides BRC^{4B} (containing 1545-LFDE-1548) and BRC^{5B} (containing 1692-WLRE-1695). However, the N-terminal peptide BRC^{5A} (containing 1671-FYTS-1674) did not exhibit significant inhibition. This may be explained by the replacement of alanine in the FHTA motif of BRC4, a small non-polar residue which is partially buried in RAD51, with a polar serine residue in the FYTS motif in BRC5.

To further explore the contribution made by the two tetrameric clusters to RAD51 binding, we constructed chimaeric peptides in which the N- or C-terminal segments from BRC4 and BRC5 were combined. Thus, peptide BRC^{45} combines the N-terminal 17 residues from BRC4 (containing 1524-FHTA-1527) with the C-terminal 18 residues from BRC5 (containing 1692-WLRE-1695), whereas BRC^{54} combines the converse segments, joining the 1671-FYTS-1674 motif from BRC5 with the 1545-LFDE-1548 from BRC4 in a 35-mer peptide. We tested whether functional FHTA and LFDE motifs in a BRC repeat are together necessary for the BRC-RAD51 interaction, because mutations that individually disrupt the FHTA or LFDE motifs in BRC4, or the natural alanine–serine substitution in the FxxA motif in BRC5, can abrogate their interaction with RAD51. Indeed, a chimaeric fusion peptide containing the N-terminus of BRC4 and C-terminus of BRC5 (BRC^{45}) phenocopied BRC4 in its behaviour as a soluble inhibitor of the BRC4–RAD51 interaction (Figure 3B). In contrast, the BRC^{54} fusion, combining the N-terminus of BRC5 with the C-terminus of BRC4, had little competitive effect, and resembled the BRC5 peptide in its behaviour. Interestingly, as predicted from the enhanced inhibitory potential of BRC^{5B} over BRC^{4B} (Figure 3A), the BRC^{45} fusion, containing the FHTA motif of BRC4 and the WLRE motif in BRC5, was more potent than BRC4 at competing the BRC4–RAD51 interaction.

The ability of wild-type, mutant or chimaeric BRC repeat peptides to compete with BRC4 for binding to RAD51 in the ELISA assay was further validated by measuring their interaction with RAD51. Biotinylated BRC peptides bound to streptavidin-coated magnetic beads were used to pull down endogenous RAD51 from human 293T cell lysates (Figure 4). After stringent washes of the bead-bound protein complexes, samples were analysed by SDS–PAGE and western blotting for RAD51. As expected, the BRC4 wild-type peptide, the tryptophan-substituted $BRC4^{WW}$ mutant, or the BRC^{45} chimera, all containing both the FHTA and LFDE motifs, efficiently pulled-down RAD51 from lysates (Figure 4A and B). The BRC5 wild-type peptide interacted only weakly with RAD51, as did the C-terminal 18-mer peptide BRC^{5B} (Figure 4C). However, neither the 17/18-mer BRC^{4A} nor BRC^{4B} peptides could pull down RAD51 from cell lysates, in agreement with a previous report (40), despite possessing the ability to compete for the BRC4–RAD51 interaction in the ELISA assay. These latter observations suggest that the C-terminal region of the BRC5 repeat, encoded in BRC^{5B}, may bind more strongly to RAD51 than the equivalent region of the BRC4 repeat, encoded in BRC^{4B}. This is surprising, because full-length BRC4 is a much stronger binder of RAD51. The failure to detect a direct interaction with the BRC^{4A} peptide, which showed competitive

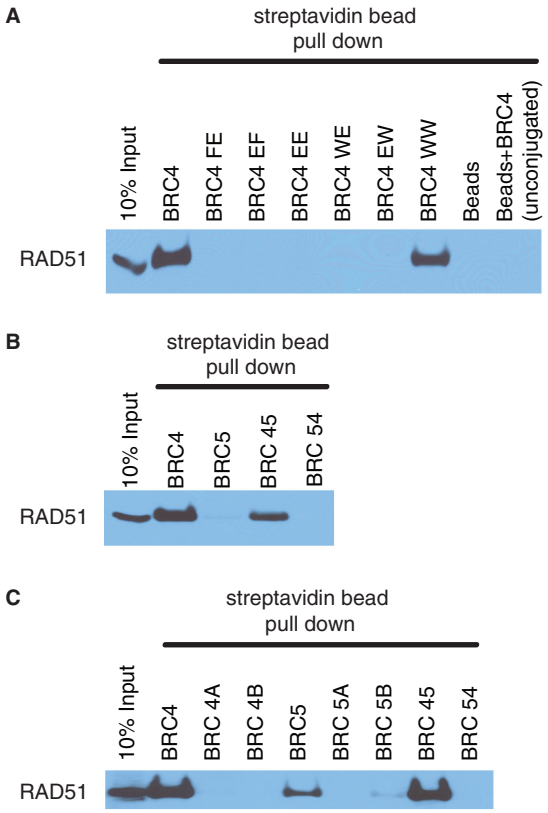

Figure 4. Presence of both binding motifs within a BRC repeat is required for strong interaction with RAD51. (**A**) A western blot of RAD51 pulled down from 293T whole-cell extract using BRC4-derived biotinylated peptides with streptavidin-coated magnetic beads. Concurring with data in Figure 2B, only a peptide containing an intact FHTA and LFDE, or combined F1524W and F1546W mutation, could directly interact with RAD51. No non-specific binding occurs to streptavidin-coated magnetic beads or addition of unconjugated BRC4 peptide. (**B**) is as in (A) and indicates very weak interaction between BRC5 and Rad51, but strong interaction with chimaeric peptide BRC^{45}. (**C**) is as in (A) and demonstrates that BRC^{5B} is the only truncated BRC peptide capable of interaction with Rad51, although only visible at an extended exposure of the blot.

inhibition in the ELISA, may reflect differences in its ability to form a stable hairpin structure in solution (i.e. in the ELISA) or when tethered on beads (i.e. in the pull-down assay).

Collectively, these results indicate that the BRC repeats use two distinct tetrameric clusters of residues in distinct secondary structural domains (in BRC4, a N-terminal β-hairpin containing FHTA, and a C-terminal α-helix containing LFDE) to bind to two separate pockets in RAD51. These tetrameric clusters jointly contribute to the ability of BRC repeats to bind RAD51. Thus, BRC4, which exhibits potent binding to RAD51, contains N- as well as C-terminal motifs that contribute to the interaction (40). In contrast, the N-terminal tetrameric motif in BRC5 may be incapable of binding to its cognate pocket in RAD51, which may account for the relatively weak affinity of this repeat for RAD51.

Co-location of FxxA and LFDE motifs within a single BRC repeat allows inhibitory and permissive modes of RAD51 regulation

To understand the functional significance of two distinct binding sites for RAD51 within a single BRC repeat, we compared the behaviour of mutant and chimaeric BRC repeats in an EMSA. RAD51 forms a nucleoprotein complex with a radiolabeled linear dsDNA substrate at an optimal base pair to RAD51 ratio of 3:1 (41). As expected, this filament is super-shifted by the addition of BRC4 at a low concentration ranging up to a 2:1 molar ratio with RAD51, reflecting the formation of a ternary complex (12,23). In contrast, ternary complex formation is inhibited at a high BRC4 concentration, greater than a 2:1 molar ratio with RAD51. Together, these behaviours reflect two functional states, in which BRC repeats are either permissive or inhibitory for RAD51 assembly on dsDNA (12,22).

Mutations in the BRC repeats perturb these functional behaviours. Point mutants that inactivate the FHTA or LFDE motifs, singly or in combination, fail to form a ternary complex with RAD51 and dsDNA in the EMSA at lower concentrations, and do not inhibit complex formation at higher concentrations (Figure 5A). This suggests that the FHTA and LFDE motifs are both required for the permissive or inhibitory interactions of BRC repeats with a RAD51-dsDNA filament. Indeed, neither the BRC5 peptide (which lacks a functional FxxA motif near its N-terminus) nor the chimaeric peptide BRC^{54} (in which the N-terminal sequence of BRC5 is fused with the C-terminal region of BRC4) exhibit either functional behaviour in the EMSA. Interestingly and in contrast, the chimeric BRC^{45} fusion peptide (which contains functional versions of the N- and C-terminal motifs) exhibits both behaviours. It forms ternary complexes with RAD51-dsDNA at up to a molar ratio of 2:1, and inhibits complex formation when present in higher amounts (Figure 5B) thus displaying similar stoichiometric effects to BRC4. Thus, we find that the co-location of the FxxA and LFDE motifs within a single BRC repeat is necessary for permissive and inhibitory effects on ternary complex formation with RAD51 and dsDNA. Since the binding site on RAD51 for the FxxA motif perturbs the interface for RAD51 oligomerization, whereas the LFDE-binding site is distant from it, this raises the possibility that the two motifs represent distinct binding modes adopted by the BRC repeats to regulate RAD51 in a manner inhibitory (FxxA) or permissive (LFDE) to its oligomerization.

The binding site on RAD51 for the LFDE motif is critical for *in vivo* function

To test the biological function of the LFDE motif, we used avian DT40 cells, a widely used model for the study of HDR (42). The BRC repeats of chicken Brca2 display homology with other known vertebrate BRC repeats in number, inter-repeat spacing and critical sequence fingerprints, including both the FxxA and LFDE modules (3). Chicken BRC3 and BRC5 deviate somewhat from their corresponding human counterparts,

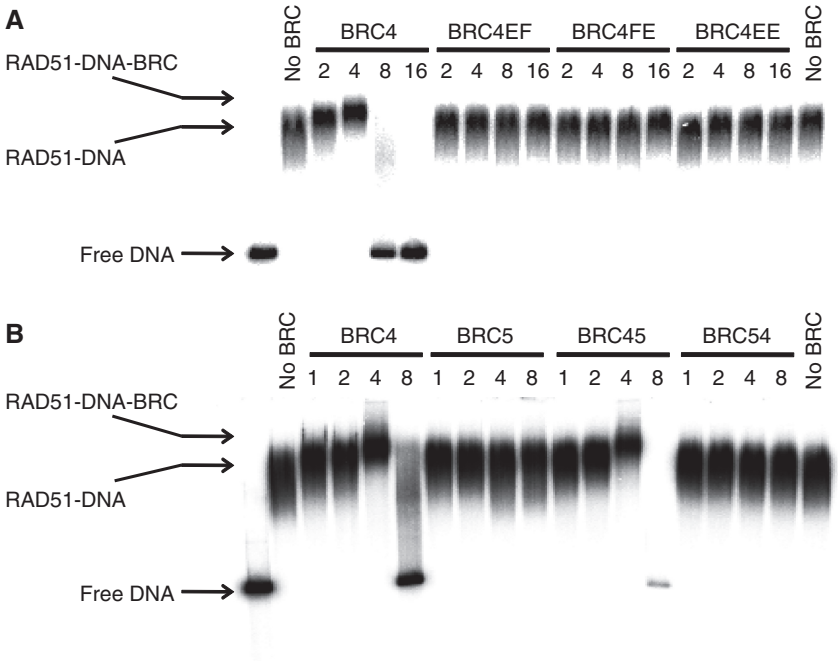

Figure 5. Functional FxxA and LFDE-like motifs are required for a BRC repeat to exert both permissive and inhibitory regulation of RAD51 nucleoprotein filament formation on dsDNA. (**A**) An EMSA assay detecting RAD51-nucleoprotein filament formation on dsDNA. BRC4 shows a concentration-dependent filament super-shift up to a 2:1 ratio with Rad51 (present at 2 μM in all lanes except lane 1 indicating mobility of unbound DNA). At super-stoichiometric BRC4 concentrations, filament formation is prevented. This behaviour is not observed in mutants of BRC4 in which either the FHTA or LFDE motif has been ablated. (**B**) is as in (A) using BRC5 and chimaeric peptides. Concentration dependent super-shift and subsequent inhibition of filament formation is observed in BRC[45], at similar concentrations to BRC4. EMSAs were performed using pre-incubation of RAD51 and BRC peptides (at indicated concentrations in micromolar) for 10 min on ice, prior to addition of radiolabeled DNA at 6 μM.

the former lacking identifiable FxxA and LFDE motifs, and the latter, containing an SLPV motif that diverges significantly from FxxA (3). Avian Rad51 is closely homologous to its human counterpart, and can be functionally replaced by wild-type human RAD51 (28), but not mutants that fail to bind chicken BRC repeats (10), suggesting functional conservation of the *in vivo* interaction between these proteins.

We defined the RAD51 residues that mediate its binding to the LFDE motif, before creating RAD51 mutants bearing alterations in these residues, to overcome technical challenges of introducing LFDE mutations in each of the eight BRC repeats of chicken Brca2. We designed mutations disrupting both polar and non-polar interactions predicted to be critical from the BRC4–RAD51 structure (3,13). Mutation R250A abrogates a putative critical salt bridge to E1548 in human BRC4, the acidic residue in the fourth position of the LFDE-motif, conserved in seven of the eight human BRC repeats (Figure 6, left panel). The two initiating hydrophobic residues in the LFDE motif (L1545 and F1546) occupy a pocket in RAD51 with the potential to be occupied by two hydrophobic residues found in conserved positions in all eight human repeats. Two conserved leucine residues, L204 and L255, within 5 Å of the 'L1545/F1546' motif at the base of the pocket are predicted to significantly contribute to its hydrophobicity (Figure 6, right panel). *In silico* mutagenesis of these two residues to glutamate predicts that the introduction of bulk and charge will

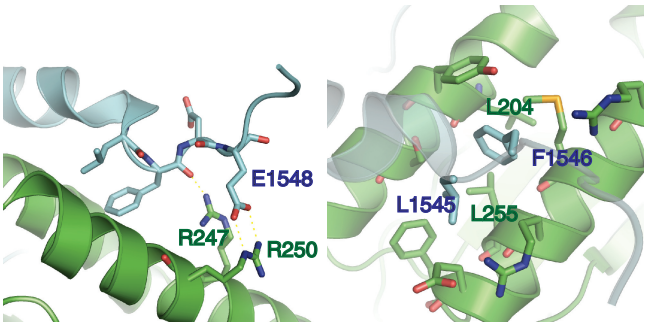

Figure 6. *In silico* mutagenesis of *Hs*RAD51 identifies polar and non-polar residues required for interaction with the LFDE motif of BRC4. A ribbon representation of BRC4 (cyan) and RAD51 (green) at the LFDE interaction site is shown. Polar contacts in the left panel indicate salt bridges between R250 in RAD51 and E1548 in BRC4 and between R247 in RAD51 and the backbone of F1546 in BRC4. The right panel identifies L204 and L255 as two hydrophobic residues at the base of the LFDE binding pocket in RAD51. All residues in stick representation are within 5Å of L1545 and F1546 in BRC4.

alter the required topology and electrostatic potential (Supplementary Figure S2) for occupation by the two hydrophobic residues in the LFDE motif of BRC repeats.

We introduced these mutations into human RAD51 expressed in DT40 cells in which endogenous Rad51 has been deleted by gene targeting (28). It has previously been shown that wild-type human RAD51, or a GFP-fluorophore tagged form, can functionally replace endogenous Rad51 in these cells, providing a robust model

widely used for the genetic analysis of RAD51 function (10). Because RAD51 is essential for cell viability, Rad51$^{-/-}$ DT40 cells were stably complemented with a conditional, Tet-repressible construct encoding wild-type human RAD51 (HsRAD51$^{Tet\ off}$), as well as with constructs encoding wild-type or mutant forms of mCherry-tagged RAD51. The addition of doxycycline eliminates HsRAD51$^{Tet\ off}$ expression, leaving only the doxycycline-resistant mCherry-tagged forms (genotypes indicated in Figure 7A). mCherry-RAD51^{WT} supports

A

	GENOTYPE		
DT40 CELL LINE	GgRad51	HsRAD51$^{Tet\ off}$	mCherry-RAD51
clone 18	+/+	not present	not present
Rad51$^{-/-}$	-/-	HsRAD51$^{Tet\ off}$	not present
RAD51^{WT}	-/-	HsRAD51$^{Tet\ off}$	wild-type
RAD51^{R250A}	-/-	HsRAD51$^{Tet\ off}$	R250A
RAD51^{LL-EE}	-/-	HsRAD51$^{Tet\ off}$	L204E, L255E
RAD51$^{LLRR-EEAA}$	-/-	HsRAD51$^{Tet\ off}$	L204E, L255E, R247A, R250A

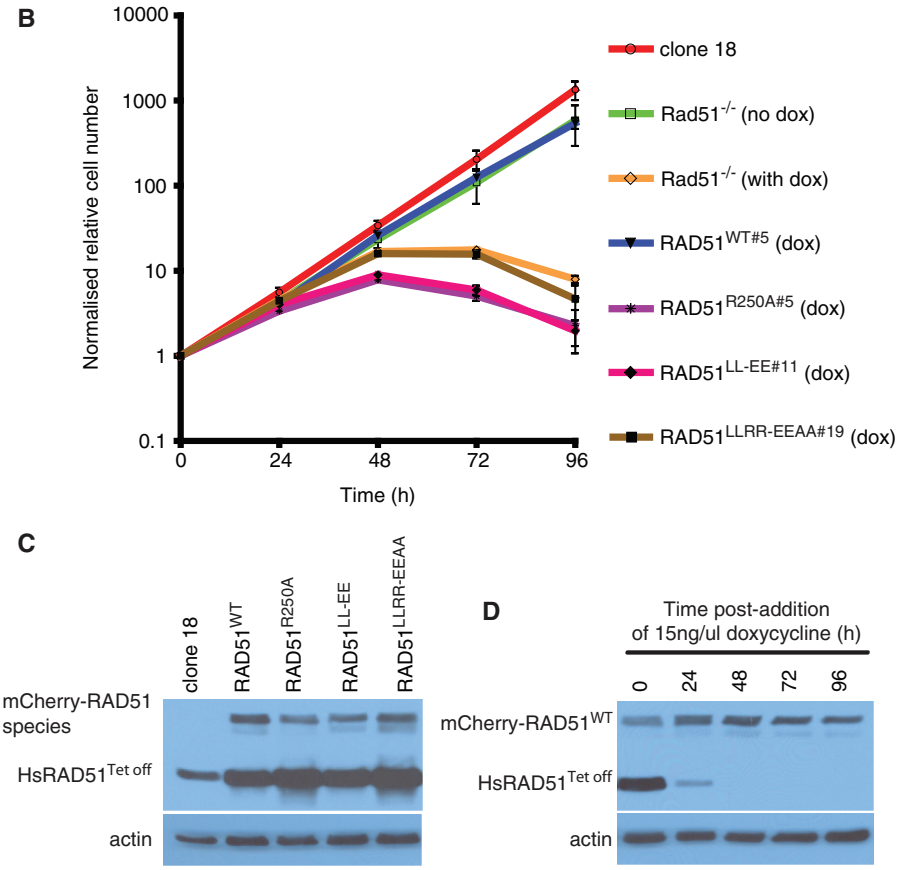

Figure 7. Insertion of point mutations into mCherry-RAD51 that disupt LFDE binding *in vivo* result in cellular lethality. (**A**) A table describing the genotypic nomenclature of cell lines generated and used in this study. HsRAD51$^{Tet\ off}$ expression can be repressed by the addition of doxycycline. (**B**) Cellular viability over 96 h of DT40 clones stably expressing mCherry-RAD51 in a Rad51$^{-/-}$/HsRAD51$^{Tet\ off}$ background after addition of doxycycline to suppress the expression of the HsRad51$^{Tet\ off}$ transgene. Wild-type clone 18 cells, Rad51$^{-/-}$ cells without doxycycline treatment and RAD51^{WT} cells with addition of doxycycline retain logarithmic growth. Mutant mCherry-RAD51 (RAD51^{R250A}, RAD51^{LL-EE} and RAD51$^{LLRR-EEAA}$) cannot rescue viability. Representative clones are shown. Each point represents the mean and SEM of viable cell counts conducted independently in triplicate. (**C**) A western blot indicating stable transfection of mCherry-RAD51 into Rad51$^{-/-}$ cells at a level comparable to endogenous chicken Rad51 in clone 18 cells, prior to addition of doxycycline. (**D**) A western blot showing time−dependent knock down of HsRad51$^{Tet\ off}$ after addition of doxycycline in a representative mCherry-RAD51^{WT}-expressing clone. HsRad51$^{Tet\ off}$ expression is undetectable at 48 h. (**E**) A pull-down assay from DT40 whole-cell extract with indicated genotypes of mCherry-tagged RAD51 and HsRad51$^{Tet\ off}$ with biotinylated-BRC4 as in Figure 4. Bio-BRC4 can pull down both species in RAD51^{WT} cells, but can only interact with HsRad51$^{Tet\ off}$ in mCherry-RAD51 mutants. (**F**) A histogram quantifying mCherry-RAD51 foci per cell in Rad51$^{-/-}$/HsRAD51$^{Tet\ off}$ cells expressing indicated mCherry-RAD51 species before and after IR, 48 h after doxycycline treatment. Each bar represents the mean and SEM of data acquired in at least 500 cells by automated microscopy. mCherry-RAD51 foci formation is apparent in RAD51^{WT} cells only with a significant induction of RAD51 foci (unpaired two-tailed *t*-test, $P < 0.0001$). Cells expressing RAD51^{R250A}, RAD51^{LL-EE}, RAD51$^{LLRR-EEAA}$ protein as the sole RAD51 species in a cell failed to show a significant induction after damage ($P = 0.0858$, 0.7573 and 0.0715, respectively, unpaired two-tailed *t*-test).

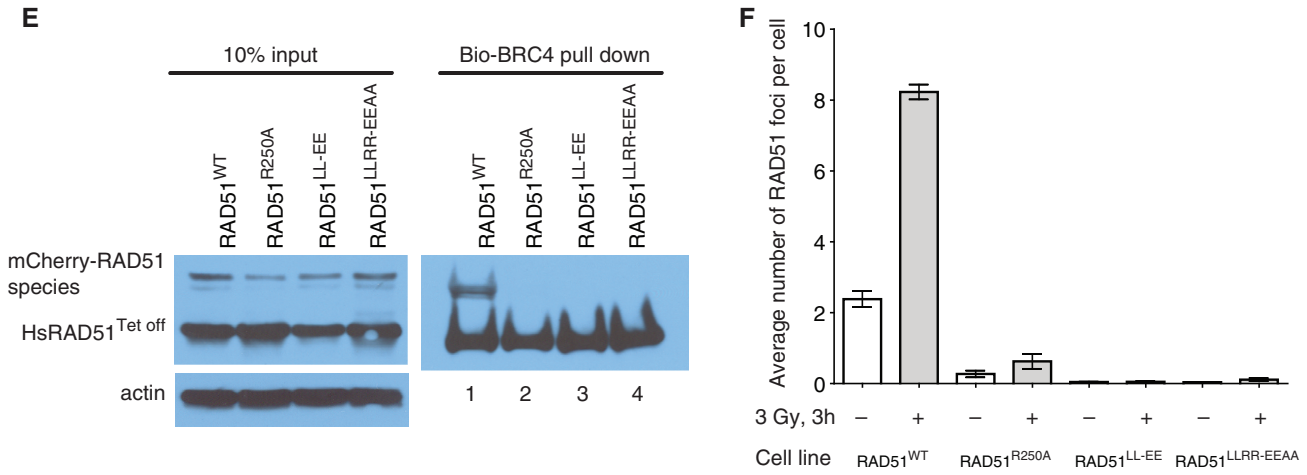

Figure 7. Continued.

HDR measured by sister chromatid exchange, widely used as a sensitive and specific test for the integrity of HDR pathways (43), at levels indistinguishable from untransfected wild-type cells (Supplementary Figure S3A). This confirms that RAD51's biological functions in HDR are unaffected by fusion to the N-terminal fluorophore.

Three mCherry-tagged RAD51 mutants were tested. The RAD51^{R250A} mutant specifically abrogates the salt bridge between the residue R250 in RAD51, and the E1548 residue in BRCA2 (Supplementary Figure S2, upper right panel). The RAD51^{LL-EE} mutant alters the hydrophobicity of the LFDE-binding pocket, substituting L204 and L255 in RAD51 for glutamate residues (Supplementary Figure S2, lower left panel). The RAD51$^{LLRR-EEAA}$ protein abrogates interactions between four residues in RAD51 and the LFDE motif in BRC repeats. The R250A, L204E and L255E mutations have been described; in addition, the R247A mutation prevents a hydrogen bond from R247 in RAD51 to the backbone of F1546 in the BRC repeat (Supplementary Figure S2, lower right panel).

Mutations in RAD51 that prevent its oligomerization and/or its interaction with BRC repeats, compromise cell viability (10). The ability of these mCherry-tagged RAD51 mutants to sustain the viability of Rad51$^{-/-}$ DT40 cells was tested. Untransfected wild-type DT40 cells (clone 18), Rad51$^{-/-}$ cells expressing HsRAD51$^{Tet\ off}$ without doxycycline treatment, and cells expressing mCherry-RAD51^{WT} were viable (Figure 7B and Supplementary Figure S3B). However, none of the three RAD51 mutants, RAD51^{R250A}, RAD51^{LL-EE} or RAD51$^{LLRR-EEAA}$, sustained viability in the presence of doxycycline, phenocopying the inviability of Rad51$^{-/-}$ cells in which the expression of HsRAD51$^{Tet\ off}$ has been switched off by doxycycline treatment (28,44). This was true of multiple, independent clones; suggesting that abrogation of the interaction between the LFDE motif in the BRC repeats of chicken Brca2, and its cognate binding pocket in RAD51, ablates RAD51 function. However, the inability of the RAD51 mutants to sustain cell viability precludes assays for sister chromatid exchange or genotoxin sensitivity.

To test the ability of mutant RAD51 to bind to BRC repeats, we chose for further analysis individual clones that expressed wild-type or mutant forms of mCherry-RAD51 at levels comparable to that of endogenous Rad51 in the parental DT40 (clone 18) cells (Figure 7C). After doxycycline treatment, wild-type HsRAD51$^{Tet\ off}$ protein was undetectable after 48 h (Figure 7D) but the expression of wild-type or mutant forms of mCherry-tagged RAD51 was unaffected. Due to the inviability of cell lines expressing mutant RAD51 alone, lysates prepared from untreated cells expressing mCherry-tagged RAD51 mutants, but retaining expression of wild-type HsRAD51$^{Tet\ off}$, were incubated with a biotinylated BRC4 peptide (Bio-BRC4) bound to streptavidin-coated magnetic beads, as in Figure 4. Bio-BRC4 is capable of pulling-down wild-type human RAD51 (HsRAD51$^{Tet\ off}$) from all lysates (Figure 7E, left-hand panel). mCherry-RAD51^{WT} can also be pulled-down by Bio-BRC4 (right-hand panel, lane 1), confirming that this interaction is unaffected by the fluorophore tag. However, the three mCherry-RAD51 mutants (RAD51^{R250A}, RAD51^{LL-EE}, RAD51$^{LLRR-EEAA}$) were defective in binding to Bio-BRC4 (left-hand panel, lanes 2–4). At high exposure, we find that small amounts of mCherry-RAD51^{R250A} can be pulled-down by Bio-BRC4, although it is clearly not the favoured binder of BRC4 when wild-type RAD51 (HsRAD51$^{Tet\ off}$) is also present in the cell lysate. This suggests that this single mutation, the least severe of those tested, may retain weak BRC repeat interaction, but this is insufficient to support its function necessary for cell viability.

Besides compromising cellular viability, mutations in RAD51 that impair its ability to interact with BRCA2 suppress its assembly in nuclear foci at sites of DNA damage (10,11,45,46). We therefore tested the ability of cells carrying wild-type and mutant forms of mCherry-RAD51 to form nuclear foci after their exposure to 3 Gy ionizing radiation (IR). These experiments were performed 48 h after the cells were treated with

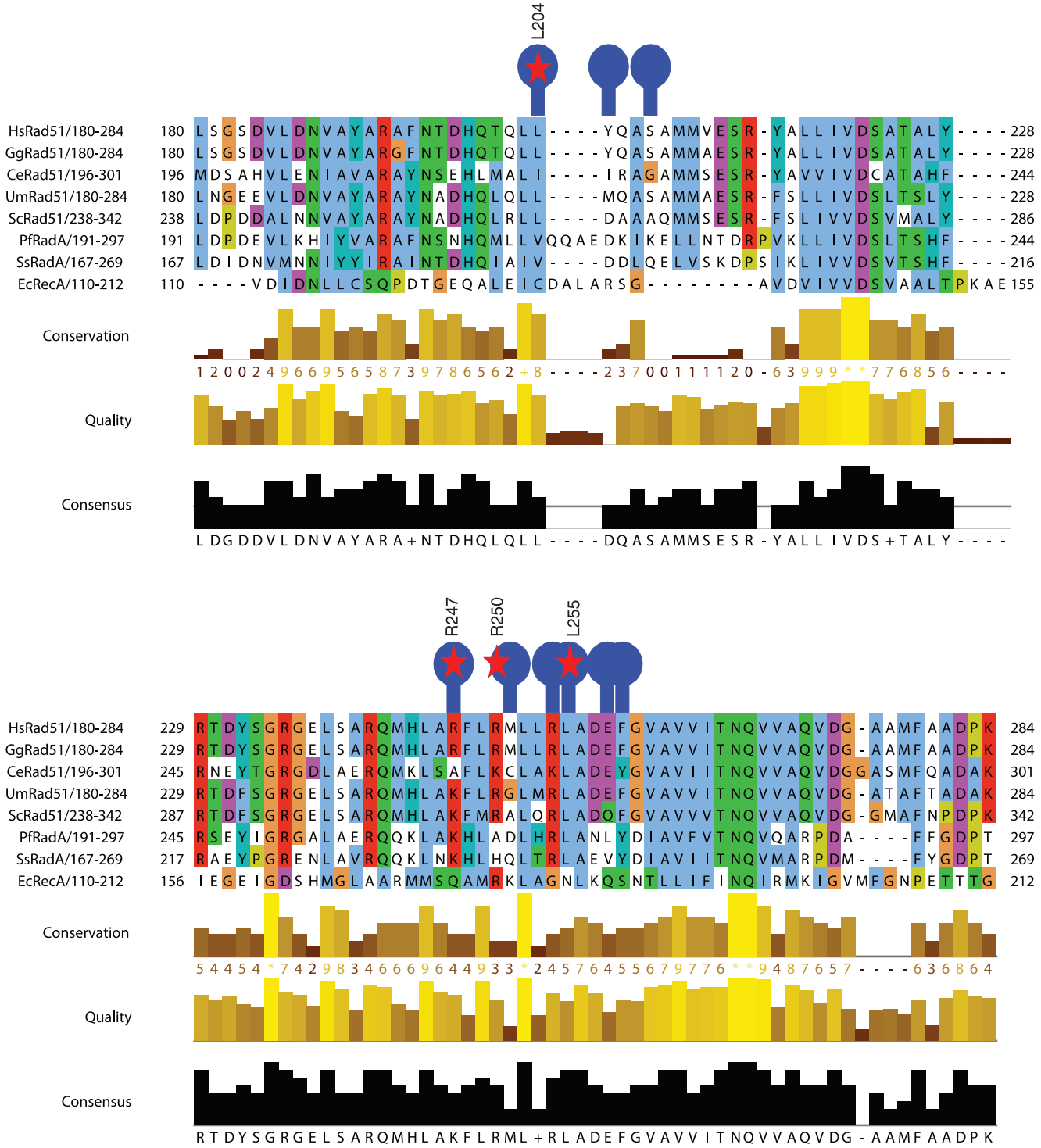

Figure 8. The LFDE binding pocket in *Hs*Rad51 is a feature of eukaryotic Rad51. A ClustalW sequence alignment is presented of *Hs*RAD51 and orthologues in other eukaryotes, archaea (RadA) and eubacteria (RecA) across human residues 180–284 and rendered with JalView. Blue circles (above sequence) indicate residues within 5Å of BRC4 residues L1545 and F1546 in *Hs*RAD51 from PDB 1N0W. Residues marked with a red star indicate residues mutated in this study (L204, R247, R250 and L255). R250A is conserved across eukaryotic Rad51 (conservatively as lysine in *C. elegans*) but also present in bacterial RecA (though not the archaeal lineage, RadA).

doxycycline, when only the wild-type or mutant mCherry-tagged RAD51 species are expressed (Figure 7D), and the cells are still fully viable (Figure 7B). Whereas mCherry-RAD51^{WT} forms IR-induced foci (quantitated by automated fluorescence microscopy in Figure 7F, with representative confocal images shown in Supplementary Figure S4), none of the three mCherry-tagged RAD51 mutants, RAD51^{R250A}, RAD51$^{LL\text{-}EE}$ or RAD51$^{LLRR\text{-}EEAA}$, exhibit foci formation. Taken together, these findings provide direct evidence that the ability of

RAD51 to bind the LFDE motif in the BRC repeats via interactions mediated by the residues R247, R250, L205 and L255 is essential for its biological functions in DNA repair. These *in vivo* findings confirm *in vitro* experiments which identify the LFDE motif as a second, previously unrecognized tetrameric motif in the BRC repeats that mediates structural and functional interactions with RAD51.

DISCUSSION

In this study, we have combined structural, cell biological, genetic and biochemical analyses to demarcate two distinct binding motifs within the BRC repeats that mediate functional interactions with RAD51 though corresponding, distinct binding pockets in RAD51. Whilst one motif, denoted FxxA, is known to inhibit RAD51 assembly by blocking oligomerization (13), we identify a second, denoted LFDE, which engages RAD51 at a distinct site distant from the oligomerization interface. We show that both motifs are required for RAD51 binding by BRC repeats. Interestingly, their co-location within a single functional BRC repeat is necessary for inhibitory and permissive regulation of RAD51 function; the motifs lack such regulatory ability in isolation. Emphasizing the mechanistic importance of these observations, mutation of the LFDE-binding pocket in RAD51 causes cellular lethality and a failure of RAD51 assembly into nuclear foci at sites of DNA breakage *in vivo*. Thus, our findings define two motifs within the BRC repeats whose structural and functional interaction with RAD51 is essential for its biological function.

The evolutionary conservation of the LFDE motif in BRC repeats from diverse organisms is striking (3). In all eight human BRC repeats (Figure 1D) as well as in almost all known BRC repeats from other organisms, the initiating dihydrophobic motif 'LF' is conserved as two hydrophobic residues. In particular, a hydrophobic residue in the second position is absolutely conserved and rare deviation only occurs if another repeat exists in the same BRCA2 orthologue that maintain this consensus (e.g. the fifteenth repeat of *Trypanosoma brucei* Brca2 that deviates from the other fourteen repeats in this respect). We note that it is this second position in BRC4 (F1546) that can be conservatively substituted with a tryptophan, with retention of RAD51 binding (Figure 2B and Figure 4A), highlighting the importance of the chemical nature of this residue.

The fourth position of the LFDE motif, comprising an acidic residue, is less strongly conserved in evolution. It forms a salt bridge with R250 in RAD51 in the BRC4-RAD51 complex (13). This residue is not always conserved, even in BRC repeats known to be strong RAD51 binders *in vitro* (e.g. human BRC3). Indeed, abrogation of the E1548A-R250 salt bridge by an R250A mutation in RAD51 significantly weakened, but did not fully abrogate, its *in vitro* interaction with BRC4 (Supplementary Figure S6D), consistent with interaction studies performed in the presence of competing wild-type RAD51 (Figure 7D). Nevertheless, the abrogation of this interaction with an R250A mutation in RAD51 phenocopies the cellular lethality and failure in RAD51 focus formation that also occurs in other RAD51 mutants, implying that even weakening of E1548-R250 salt bridge is sufficient to disrupt BRC–RAD51 interaction *in vivo*.

The conservation of the LFDE motif in the BRC repeats of BRCA2 orthologues is mirrored by the conservation of its cognate binding-pocket in RAD51 orthologues. Interestingly, this conservation extends to yeast Rad51 and even to archaeal RadA. Because these organisms lack BRCA2, our findings raise the possibility that the pocket is used for interactions with alternative binding partners (8,47).

The conservation of RAD51 R250, which forms a salt bridge with the E1548 residue in the LFDE motif of BRC4, is of particular interest. R250 is strongly conserved as R177 in *E. coli* RecA, providing insights into its potential role in RAD51 (Supplementary Figure S5, left panels) (5,6). The recently reported structure of RecA assembled on DNA substrates shows that R177 may be important for oligomerization on both ssDNA and dsDNA, and in interaction with the phosphate backbone of DNA (48). However, such interactions do not appear to be essential for RAD51 assembly. Thus, a mutant form of RAD51 carrying an R250A substitution (Supplementary Figure S6A) showed intact interaction with both ss and dsDNA (Supplementary Figure S6B) and was capable of oligomerization as assessed by GST-pull down (Supplementary Figure S6C).

In *Ec* RecA, R177 is capable of forming a salt bridge with E155 of an adjacent RecA protomer in a nucleoprotein filament (Supplementary Figure S5B and C) but not in the absence of DNA (Supplementary Figure S5A) (48). E155 however is not conserved in eukaryotic RAD51. Instead, a structural alignment of the BRC4-RAD51 complex on the core catalytic domain of RecA protomers in oligomeric states both on and off DNA suggests that the E1548-R250 salt bridge between BRC4 and RAD51 structurally mimics the E155-R177 contact between protomers in a RecA filament (Supplementary Figure S5, right panels). This is reminiscent of the structural conservation between 27-IMRL-30 at the protomer interface in *Ec*RecA, and the 1524-FHTA-1527 motif in BRC4 of human BRCA2 (13). We are tempted to speculate that the E1548-R250 salt bridge may represent a second example of 'molecular mimicry' by BRC repeats of contacts between RecA protomers, which is used in higher species for the regulation of RAD51 by BRCA2 (13).

It is unclear, however, whether the R177-E155 salt bridge between RecA promoters is structurally conserved between protomers in RAD51 filaments, in the absence of any high-resolution crystal structures. It is clear from crystallographic analysis of orthologous proteins and low-resolution electron microscopic analysis of nucleoprotein filaments that R250 in RAD51 does localize at an interface (22,49–52). It is conceivable that, like its bacterial counterpart, R250 functions in a buried salt bridge in the human RAD51 filament as a 'molecular clasp' at a RAD51 interface in a nucleoprotein filament (48).

If correct, this salt bridge might serve a stabilizing role in RAD51 assembly, directly or via the RAD51 ATPase activity, that could be regulated by BRC repeats capable of 'mimicking' this interaction using an LFDE interactive mode. Thus, our findings suggest evolutionary links in the structure of protein–protein interactions essential for the regulation of RAD51 assembly on DNA substrates during HDR that warrant further investigation.

SUPPLEMENTARY DATA

Supplementary Data are available at NAR Online.

ACKNOWLEDGEMENTS

We thank Dr Mahmud Shivji for critical guidance and advice on electrophoretic mobility shift assays, Dr Anand Jeyasekharan for help with automated microscopy, Meredith Roberts-Thomson for assistance with ELISA assays, Jane Savill for technical help with protein purification and Simon McCallum (Department of Medicine, University of Cambridge) for carrying out FACS analysis on cell lines.

FUNDING

UK Medical Research Council, which supports the work in A.R.V.'s laboratory (PhD studentship to E.R.). Funding for open access charge: Medical Research Council, UK.

Conflict of interest statement. None declared.

REFERENCES

1. Kojic,M., Kostrub,C.F., Buchman,A.R. and Holloman,W.K. (2002) BRCA2 homolog required for proficiency in DNA repair, recombination, and genome stability in Ustilago maydis. *Mol. Cell*, **10**, 683–691.
2. Moynahan,M.E., Pierce,A.J. and Jasin,M. (2001) BRCA2 is required for homology-directed repair of chromosomal breaks. *Mol. Cell*, **7**, 263–272.
3. Lo,T., Pellegrini,L., Venkitaraman,A.R. and Blundell,T.L. (2003) Sequence fingerprints in BRCA2 and RAD51: implications for DNA repair and cancer. *DNA Repair*, **2**, 1015–1028.
4. Venkitaraman,A.R. (2009) Linking the cellular functions of BRCA genes to cancer pathogenesis and treatment. *Annu. Rev. Pathol.*, **4**, 461–487.
5. Shinohara,A., Ogawa,H., Matsuda,Y., Ushio,N., Ikeo,K. and Ogawa,T. (1993) Cloning of human, mouse and fission yeast recombination genes homologous to RAD51 and recA. *Nat. Genet.*, **4**, 239–243.
6. Ogawa,T., Shinohara,A., Nabetani,A., Ikeya,T., Yu,X., Egelman,E.H. and Ogawa,H. (1993) RecA-like recombination proteins in eukaryotes: functions and structures of RAD51 genes. *Cold Spring Harb. Symp. Quant. Biol.*, **58**, 567–576.
7. West,S.C. (2003) Molecular views of recombination proteins and their control. *Nat. Rev. Mol. Cell Biol.*, **4**, 435–445.
8. San Filippo,J., Sung,P. and Klein,H. (2008) Mechanism of eukaryotic homologous recombination. *Annu. Rev. Biochem.*, **77**, 229–257.
9. Li,X. and Heyer,W.D. (2008) Homologous recombination in DNA repair and DNA damage tolerance. *Cell Res.*, **18**, 99–113.
10. Yu,D.S., Sonoda,E., Takeda,S., Huang,C.L., Pellegrini,L., Blundell,T.L. and Venkitaraman,A.R. (2003) Dynamic control of Rad51 recombinase by self-association and interaction with BRCA2. *Mol. Cell*, **12**, 1029–1041.
11. Yuan,S.S., Lee,S.Y., Chen,G., Song,M., Tomlinson,G.E. and Lee,E.Y. (1999) BRCA2 is required for ionizing radiation-induced assembly of Rad51 complex in vivo. *Cancer Res.*, **59**, 3547–3551.
12. Davies,A.A., Masson,J.Y., McIlwraith,M.J., Stasiak,A.Z., Stasiak,A., Venkitaraman,A.R. and West,S.C. (2001) Role of BRCA2 in control of the RAD51 recombination and DNA repair protein. *Mol. Cell*, **7**, 273–282.
13. Pellegrini,L., Yu,D.S., Lo,T., Anand,S., Lee,M., Blundell,T.L. and Venkitaraman,A.R. (2002) Insights into DNA recombination from the structure of a RAD51-BRCA2 complex. *Nature*, **420**, 287–293.
14. Carreira,A., Hilario,J., Amitani,I., Baskin,R.J., Shivji,M.K., Venkitaraman,A.R. and Kowalczykowski,S.C. (2009) The BRC repeats of BRCA2 modulate the DNA-binding selectivity of RAD51. *Cell*, **136**, 1032–1043.
15. Shivji,M.K., Mukund,S.R., Rajendra,E., Chen,S., Short,J.M., Savill,J., Klenerman,D. and Venkitaraman,A.R. (2009) The BRC repeats of human BRCA2 differentially regulate RAD51 binding on single- versus double-stranded DNA to stimulate strand exchange. *Proc. Natl Acad. Sci. USA*, **106**, 13254–13259.
16. Bignell,G., Micklem,G., Stratton,M.R., Ashworth,A. and Wooster,R. (1997) The BRC repeats are conserved in mammalian BRCA2 proteins. *Hum. Mol. Genet.*, **6**, 53–58.
17. Bork,P., Blomberg,N. and Nilges,M. (1996) Internal repeats in the BRCA2 protein sequence. *Nat. Genet.*, **13**, 22–23.
18. Takata,M., Tachiiri,S., Fujimori,A., Thompson,L.H., Miki,Y., Hiraoka,M., Takeda,S. and Yamazoe,M. (2002) Conserved domains in the chicken homologue of BRCA2. *Oncogene*, **21**, 1130–1134.
19. Chen,C.F., Chen,P.L., Zhong,Q., Sharp,Z.D. and Lee,W.H. (1999) Expression of BRC repeats in breast cancer cells disrupts the BRCA2-Rad51 complex and leads to radiation hypersensitivity and loss of G(2)/M checkpoint control. *J. Biol. Chem.*, **274**, 32931–32935.
20. Chen,P.L., Chen,C.F., Chen,Y., Xiao,J., Sharp,Z.D. and Lee,W.H. (1998) The BRC repeats in BRCA2 are critical for RAD51 binding and resistance to methyl methanesulfonate treatment. *Proc. Natl Acad. Sci. USA*, **95**, 5287–5292.
21. Wong,A.K., Pero,R., Ormonde,P.A., Tavtigian,S.V. and Bartel,P.L. (1997) RAD51 interacts with the evolutionarily conserved BRC motifs in the human breast cancer susceptibility gene brca2. *J. Biol. Chem.*, **272**, 31941–31944.
22. Galkin,V.E., Esashi,F., Yu,X., Yang,S., West,S.C. and Egelman,E.H. (2005) BRCA2 BRC motifs bind RAD51-DNA filaments. *Proc. Natl Acad. Sci. USA*, **102**, 8537–8542.
23. Shivji,M.K., Davies,O.R., Savill,J.M., Bates,D.L., Pellegrini,L. and Venkitaraman,A.R. (2006) A region of human BRCA2 containing multiple BRC repeats promotes RAD51-mediated strand exchange. *Nucleic Acids Res.*, **34**, 4000–4011.
24. Davies,O.R. and Pellegrini,L. (2007) Interaction with the BRCA2 C terminus protects RAD51-DNA filaments from disassembly by BRC repeats. *Nat. Struct. Mol. Biol.*, **14**, 475–483.
25. Esashi,F., Galkin,V.E., Yu,X., Egelman,E.H. and West,S.C. (2007) Stabilization of RAD51 nucleoprotein filaments by the C-terminal region of BRCA2. *Nat. Struct. Mol. Biol.*, **14**, 468–474.
26. Ayoub,N., Rajendra,E., Su,X., Jeyasekharan,A.D., Mahen,R. and Venkitaraman,A.R. (2009) The carboxyl terminus of Brca2 links the disassembly of Rad51 complexes to mitotic entry. *Curr. Biol.*, **19**, 1075–1085.
27. San Filippo,J., Chi,P., Sehorn,M.G., Etchin,J., Krejci,L. and Sung,P. (2006) Recombination mediator and Rad51 targeting activities of a human BRCA2 polypeptide. *J. Biol. Chem.*, **281**, 11649–11657.
28. Sonoda,E., Sasaki,M.S., Buerstedde,J.M., Bezzubova,O., Shinohara,A., Ogawa,H., Takata,M., Yamaguchi-Iwai,Y. and Takeda,S. (1998) Rad51-deficient vertebrate cells accumulate chromosomal breaks prior to cell death. *EMBO J.*, **17**, 598–608.
29. Niedzwiedz,W., Mosedale,G., Johnson,M., Ong,C.Y., Pace,P. and Patel,K.J. (2004) The Fanconi anaemia gene FANCC promotes homologous recombination and error-prone DNA repair. *Mol. Cell*, **15**, 607–620.

30. Baker,N.A., Sept,D., Joseph,S., Holst,M.J. and McCammon,J.A. (2001) Electrostatics of nanosystems: application to microtubules and the ribosome. *Proc. Natl Acad. Sci. USA*, **98**, 10037–10041.
31. Kleinjung,J. and Fraternali,F. (2005) POPSCOMP: an automated interaction analysis of biomolecular complexes. *Nucleic Acids Res.*, **33**, W342–W346.
32. Larkin,M.A., Blackshields,G., Brown,N.P., Chenna,R., McGettigan,P.A., McWilliam,H., Valentin,F., Wallace,I.M., Wilm,A., Lopez,R. *et al.* (2007) Clustal W and Clustal X version 2.0. *Bioinformatics*, **23**, 2947–2948.
33. Clamp,M., Cuff,J., Searle,S.M. and Barton,G.J. (2004) The Jalview Java alignment editor. *Bioinformatics*, **20**, 426–427.
34. Shin,D.S., Pellegrini,L., Daniels,D.S., Yelent,B., Craig,L., Bates,D., Yu,D.S., Shivji,M.K., Hitomi,C., Arvai,A.S. *et al.* (2003) Full-length archaeal Rad51 structure and mutants: mechanisms for RAD51 assembly and control by BRCA2. *EMBO J.*, **22**, 4566–4576.
35. Jones,S. and Thornton,J.M. (1996) Principles of protein-protein interactions. *Proc. Natl Acad. Sci. USA*, **93**, 13–20.
36. Jones,S. and Thornton,J.M. (1997) Analysis of protein-protein interaction sites using surface patches. *J. Mol. Biol.*, **272**, 121–132.
37. Bogan,A.A. and Thorn,K.S. (1998) Anatomy of hot spots in protein interfaces. *J. Mol. Biol.*, **280**, 1–9.
38. Clackson,T. and Wells,J.A. (1995) A hot spot of binding energy in a hormone-receptor interface. *Science*, **267**, 383–386.
39. Thorslund,T., Esashi,F. and West,S.C. (2007) Interactions between human BRCA2 protein and the meiosis-specific recombinase DMC1. *EMBO J.*, **26**, 2915–2922.
40. Nomme,J., Takizawa,Y., Martinez,S.F., Renodon-Corniere,A., Fleury,F., Weigel,P., Yamamoto,K., Kurumizaka,H. and Takahashi,M. (2008) Inhibition of filament formation of human Rad51 protein by a small peptide derived from the BRC-motif of the BRCA2 protein. *Genes Cells*, **13**, 471–481.
41. Baumann,P., Benson,F.E. and West,S.C. (1996) Human Rad51 protein promotes ATP-dependent homologous pairing and strand transfer reactions in vitro. *Cell*, **87**, 757–766.
42. Yamazoe,M., Sonoda,E., Hochegger,H. and Takeda,S. (2004) Reverse genetic studies of the DNA damage response in the chicken B lymphocyte line DT40. *DNA Repair*, **3**, 1175–1185.
43. Sonoda,E., Sasaki,M.S., Morrison,C., Yamaguchi-Iwai,Y., Takata,M. and Takeda,S. (1999) Sister chromatid exchanges are mediated by homologous recombination in vertebrate cells. *Mol. Cell Biol.*, **19**, 5166–5169.
44. Su,X., Bernal,J.A. and Venkitaraman,A.R. (2008) Cell-cycle coordination between DNA replication and recombination revealed by a vertebrate N-end rule degron-Rad51. *Nat. Struct. Mol. Biol.*, **15**, 1049–1058.
45. Haaf,T., Golub,E.I., Reddy,G., Radding,C.M. and Ward,D.C. (1995) Nuclear foci of mammalian Rad51 recombination protein in somatic cells after DNA damage and its localization in synaptonemal complexes. *Proc. Natl Acad. Sci. USA*, **92**, 2298–2302.
46. Yu,V.P., Koehler,M., Steinlein,C., Schmid,M., Hanakahi,L.A., van Gool,A.J., West,S.C. and Venkitaraman,A.R. (2000) Gross chromosomal rearrangements and genetic exchange between nonhomologous chromosomes following BRCA2 inactivation. *Genes Dev.*, **14**, 1400–1406.
47. Sung,P., Krejci,L., Van Komen,S. and Sehorn,M.G. (2003) Rad51 recombinase and recombination mediators. *J. Biol. Chem.*, **278**, 42729–42732.
48. Chen,Z., Yang,H. and Pavletich,N.P. (2008) Mechanism of homologous recombination from the RecA-ssDNA/dsDNA structures. *Nature*, **453**, 489–484.
49. Conway,A.B., Lynch,T.W., Zhang,Y., Fortin,G.S., Fung,C.W., Symington,L.S. and Rice,P.A. (2004) Crystal structure of a Rad51 filament. *Nat. Struct. Mol. Biol.*, **11**, 791–796.
50. Galkin,V.E., Wu,Y., Zhang,X.P., Qian,X., He,Y., Yu,X., Heyer,W.D., Luo,Y. and Egelman,E.H. (2006) The Rad51/RadA N-terminal domain activates nucleoprotein filament ATPase activity. *Structure*, **14**, 983–992.
51. Ogawa,T., Yu,X., Shinohara,A. and Egelman,E.H. (1993) Similarity of the yeast RAD51 filament to the bacterial RecA filament. *Science*, **259**, 1896–1899.
52. Yu,X., Jacobs,S.A., West,S.C., Ogawa,T. and Egelman,E.H. (2001) Domain structure and dynamics in the helical filaments formed by RecA and Rad51 on DNA. *Proc. Natl Acad. Sci. USA*, **98**, 8419–8424.